A New Calorimeter for Simultaneous Measurements of Loading and Heats of Adsorption from Gas Mixtures

ARTICLE *in* LANGMUIR · JANUARY 1999

Impact Factor: 4.46 · DOI: 10.1021/la980946a

3 AUTHORS, INCLUDING:

Raymond J. Gorte
University of Pennsylvania
413 PUBLICATIONS **18,057** CITATIONS

SEE PROFILE

Alan L. Myers
University of Pennsylvania
93 PUBLICATIONS **5,071** CITATIONS

SEE PROFILE

A New Calorimeter for Simultaneous Measurements of Loading and Heats of Adsorption from Gaseous Mixtures

Flor Siperstein, Raymond J. Gorte, and Alan L. Myers*

Department of Chemical Engineering, University of Pennsylvania, Philadelphia, Pennsylvania 19104-6393

Received July 28, 1998. In Final Form: November 16, 1998

A new calorimeter has been designed to measure isosteric heats of adsorption from gaseous mixtures with simultaneous measurements of loading and composition. The combined measurements at a single reference temperature provide complete thermodynamic information on the equilibrium behavior of a binary mixture. The components of a binary mixture are dosed alternately so that the individual isosteric heats can be determined from two successive measurements. The necessity of establishing equilibrium within 30 min of adding a dose of gas placed stringent limitations on the design of the sample cell. The attainment of equilibrium was verified by reversing the order of contact of the components of the mixture. The composition of the equilibrium gas phase is determined with a leak valve to a mass spectrometer in order to minimize perturbations of the system.

1. Introduction

Optimal design of pressure-swing adsorption (PSA) units for separation of gaseous mixtures is based on experimental equilibrium data for loading and selectivity as a function of pressure, temperature, and composition. The modeling of thermal effects accompanying adsorption and desorption cycles requires an energy balance based on the heats of adsorption of individual components of the mixture. Measurements of loading, selectivity, and heats using conventional methods are expensive and difficult. Heats of adsorption of pure gases, which are usually obtained from isotherms using the Clapeyron equation, are unreliable unless extra precautions are taken to ensure reversibility and reproducibility. The calculation of mixture heats from extensions of the Clapeyron equation is impractical.[1] However, we have recently demonstrated that both adsorption isotherms and multicomponent heats of adsorption can be measured accurately and quickly in a single, inexpensive instrument.[2] This paper summarizes the design criteria and construction of our combination calorimeter−volumetric apparatus in sufficient detail to reproduce our instrument, with numerous helpful suggestions for avoiding some of the pitfalls associated with adsorption calorimetry.

2. Design Criteria

The desired equilibrium information for adsorbed mixtures is the pressure and composition of the gas phase above the adsorbent for a given loading, as well as the heat evolved for differential increases in the loading. Because we considered direct, calorimetric measurements of differential heats to be more reliable than differentiation of isotherms at various temperatures, the instrument was built around a Tian−Calvet calorimeter. Practical limitations on the ability to integrate the heat flux in the calorimeter as a function of time required that equilibrium be established in 30 min or less. In order to avoid significant perturbations of the system during measurement of the gas-phase composition, we used a quadrupole mass spectrometer.

The necessity of establishing equilibrium within 30 min of changing the sample loading placed a stringent limitation on the design. First, we excluded adsorption systems for which diffusion of one of the components was too slow to establish equilibrium quickly. For most systems of importance in PSA, which requires reversible adsorption, this is not a severe limitation. To minimize concentration gradients in the sample bed, a thin layer of adsorbent (≈3 mm) was placed on the bottom of the calorimeter cell. In addition to minimizing the diffusion time within the bed, the use of a thin adsorbent bed also decreased the time necessary for the heat generated by adsorption to be collected by the thermopiles at the walls of the cell. The size of the calorimeter cell, a 1-in. cube, represents a compromise between the sensitivity of the instrument, which increases with the amount of adsorbent, and the rate of equilibration, which decreases with the cell size. Equilibration within the adsorbent bed is rapid for this configuration: based on a typical Knudsen diffusion coefficient of 0.01 cm^2/s for mixing in the gas phase of the sample bed, the mixing time is $L^2/D \approx (0.3)^2\ cm^2/(0.01\ cm^2/s = 9$ s. While diffusion coefficients within the particles making up the adsorbent may be much smaller than the Knudsen coefficient, particularly for a zeolite, the sizes of crystals making up a typical zeolite sample are also quite small. Even for crystallites on the order of 1 mm, the diffusion coefficient would have to be significantly below 10^{-8} cm^2/s for mixing to be a limiting factor for equilibration.

The major limitation for the attainment of adsorption equilibrium is gas-phase mixing in the region above the sample. On the basis of a typical gas-phase diffusion coefficient of 0.1 cm^2/s, a tube length of even 10 cm will result in mixing times of 1000 s. This imposes significant challenges on the instrument design. While imposed circulation would alleviate this problem, forced flow would also complicate the design of the calorimeter because of convective heat losses. The maximum distance within our apparatus (from the bottom of the sample cell to the diaphragm of the pressure transducer) was approximately 10 cm. The pressure transducer was chosen for its small dead volume. The leak valve for the composition measurements was welded directly on the top of the cell to minimize the dimensions of the apparatus. These design

(1) Sircar, S. *J. Chem. Soc., Faraday Trans. 1* **1985**, *81*, 1527.
(2) Dunne, J. A.; Rao, M.; Sircar, S.; Gorte, R. J.; Myers, A. L. *Langmuir* **1997**, *13*, 4333.

10.1021/la980946a CCC: $18.00
Published on Web 01/21/1999

criteria could only be met by a custom-made calorimeter. The total equipment cost of the apparatus, of which the major components are the residual gas analyzer (RGA), the pressure transducer, the thermopiles, and the computer, was about $20,000.

3. Theory

The isosteric heat of adsorption is defined as the difference between the partial molar enthalpies in the gas and adsorbed phases:

$$Q_{st} = \bar{h}^g - \bar{h}^a \tag{1}$$

Thus, Q_{st} is the heat of *desorption*, even though it is not a heat but the difference of two state functions, but the name is well established. The actual heat measured in a particular calorimeter must be related to the thermodynamic definition of isosteric heat in eq 1.

Idealized Calorimeter. An idealized batch calorimeter consists of a dosing cell, sample cell, and valve between the dosing cell and sample cell completely enclosed in an isothermal calorimeter at temperature T_0. At the start, the valve is closed, both cells are at temperature T_0, the pressure in the dosing loop is P_d, and the pressure in the sample cell is P_c, with $P_d > P_c$.

When the value is opened, an increment of gas expands from the dosing cell into the sample cell and a portion of the increment adsorbs. The total energy is

$$U = U^g + U^a = u^g n^g + u^a n^a \tag{2}$$

The total energy U includes that of the adsorbent, the walls of the sample cell and dosing cell, and the valve. However, since the temperature is fixed at T_0, these energies are omitted from eq 2 because they are constant and do not contribute to the change in energy. The total amount of gas in both cells is n^g. The differential of the total energy is

$$dU = u^g\, dn^g + n^g\, du^g + u^a\, dn^a + n^a\, du^a \tag{3}$$

where dU refers to the differential energy change after attainment of adsorption equilibrium. Because the temperature is T_0 before and after adsorption, $du^g = 0$ and

$$dU = u^g\, dn^g + u^a\, dn^a + n^a\, du^a \tag{4}$$

The mass balance is

$$n^g + n^a = \text{constant} \tag{5}$$

so

$$dn^g = -dn^a \tag{6}$$

Substituting eq 6 into eq 4:

$$dU = -u^g\, dn^a + u^a\, dn^a + n^a\, du^a \tag{7}$$

The first law for the combined closed system consisting of the dosing cell, sample cell, and valve is

$$dU = dQ \tag{8}$$

where dQ is the heat adsorbed by the combined system. For adsorption, dQ is a negative quantity. Combining eqs 7 and 8

$$-dQ = u^g\, dn^a - u^a\, dn^a - n^a\, du^a \tag{9}$$

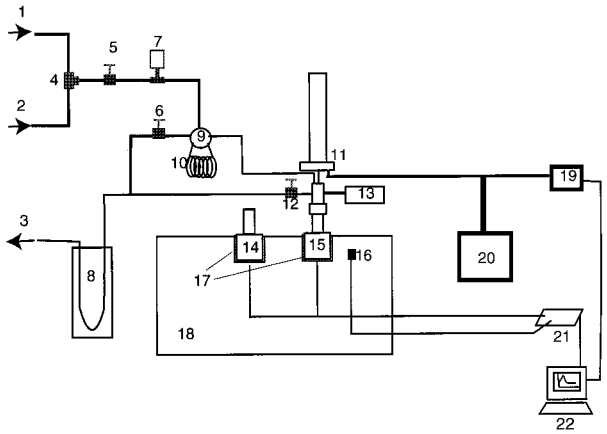

Figure 1. Schematic of the calorimeter and auxiliary equipment.

Table 1. Key to Figure 1

no.	description	model no.
1	gas 1 inlet	
2	gas 2 inlet	
3	to vacuum pump	
4	three-way valve	
5	inlet valve to the dosing loop	
6	outlet valve from the dosing loop	
7	pressure transducer for the dosing loop	MKS 626A
8	liquid nitrogen trap	
9	Valco six-way valve	
10	calibrated dosing loop (10 cm^3)	
11	variable leak valve	Granville-Phillips 203
12	cell outlet valve	
13	pressure transducer for the cell	Omega PX425
14	reference cell	
15	calorimeter cell	
16	K-type thermocouple	
17	thermopiles	International Thermal Instrument C-783
18	heat sink (aluminum block)	
19	mass spectrometer (RGA)	Leybold Inficon TSP C100F
20	turbopump	Balzers TSU062
21	data acquisition board	
22	computer	

or

$$-\frac{dQ}{dn^a} = u^g - \left[u^a + n^a \frac{du^a}{dn^a}\right] \tag{10}$$

Because $h^a \approx u^a$ and $h^g = u^g + zRT_0$, comparison of eqs 1 and 10 gives

$$Q_{st} = -\frac{dQ}{dn^a} + zRT_0 \tag{11}$$

This result was derived by Hill.[3] The first term is the differential heat measured by the idealized calorimeter, and the second term is the difference between the enthalpy and the internal energy in the equilibrium gas phase. $z = PV/RT$, the compressibility factor in the gas phase, is close to unity for subatmospheric measurements of isosteric heat. The RT_0 term at 25 °C is 2.5 kJ/mol, and typical isosteric heats of adsorption are in the range 10−50 kJ/mol.

Practical Calorimeter. In the idealized calorimeter, the temperature of the gas in the sample loop decreases upon expansion while the temperature of the gas in the

(3) Hill, T. L. *J. Chem. Phys.* **1949**, *17* (6), 520.

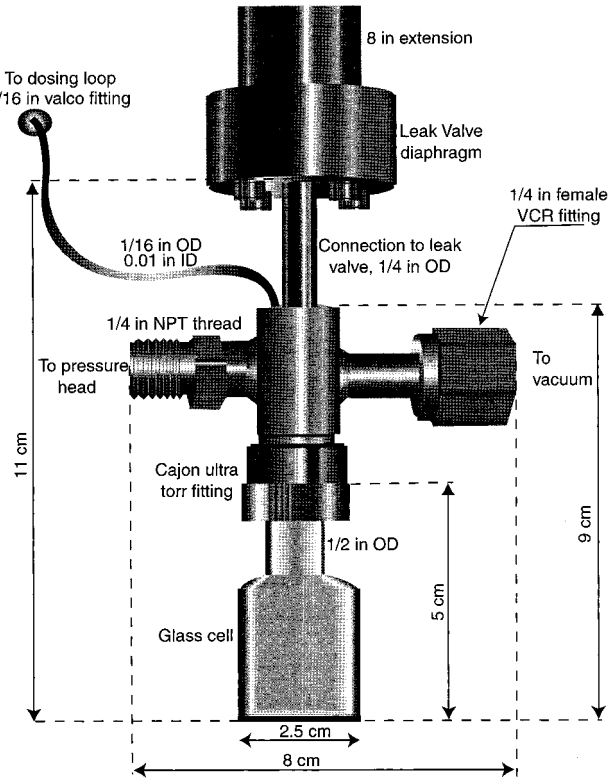

Figure 2. Picture of the glass sample cell and connections to the pressure head, vacuum line, dosing loop, and RGA leak valve. The glass sample cell is surrounded by thermopiles (not shown) set into an aluminum heat sink.

sample cell increases as it is compressed by the incoming gas. In the absence of adsorption, heat is absorbed by the dosing loop and heat is liberated by the sample cell until the pressures equalize and the temperature returns to T_0. For a perfect gas, the two effects cancel because the enthalpy of a perfect gas is a function only of temperature.

Our design is a modification of the idealized calorimeter in which only the sample cell is placed in the calorimeter. Because the dosing loop and valve are external to the calorimeter, adding a dose of gas to the sample cell generates an exothermic heat of compression in the sample cell which is not cancelled by absorption of heat in the dosing loop. The spurious heat of compression calculated from eq 12 is subtracted from the total heat registered by the calorimeter in order to obtain the heat of adsorption.

4. Description of Instrument

A diagram of the calorimeter apparatus is shown in Figure 1; the components are described in Table 1. A picture of the sample cell and its connections is shown in Figure 2. The glass (Pyrex) cube is the sample cell for the adsorbent and adsorbate. The use of glass to minimize heat conduction through the top of the cell is a crucial element of the design. The glass cube is surrounded on all four sides and on the bottom by square thermal flux meters (not shown in the picture) obtained from the International Thermal Instrument Company, Del Mar, CA. Each thermopile is a 1-in.^{2} polyimide plate with about 100 embedded thermocouples for detecting temperature differences across the plate. The five thermopiles were connected in series and a similar set in the reference cell was connected in opposition to improve baseline stability. The combined signal from these transducers was input to an amplifier on the data acquisition board of a computer. The sample cell slides into cubical holes cut into an aluminum block (27 × 18 × 10 cm, mass 13 kg). A silicone-based heat-sink compound was used to ensure good thermal contact between the Al block and the transducers and between the transducers and the pyrex cell.

The cubical glass cell shown in Figure 2 was made with a $^1/_2$-in. glass tube on the top which was inserted into a Cajon fitting, which provides a vacuum seal by compression of a Viton O-ring. The Cajon fitting connects to a custom-made *T* connection onto which are welded the leak valve, the pressure head, the connection to vacuum, and the 0.01-in. bore tube from the dosing loop. The leak valve is connected through a $^1/_4$-in.-o.d. stainless-steel tube; the pressure head is connected through a $^1/_4$-in. δ NPT fitting; the valve that opens to vacuum is connected through a $^1/_4$-in. VCR fitting. The pressure head was chosen for its small dead space (1.2 cm^3). The total dead space is 20.6 cm^3 for the (empty) sample cell, the dead space inside the pressure head, and the lines to vacuum, the dosing loop, and the RGA leak valve.

Gas was introduced to the sample cell from the dosing loop using a six-port Valco sampling valve connected to a small bore (0.01-in.-i.d.) tube. The small diameter of the tube prevents backmixing of the mixture into the dosing loop. This tube enters the *T*-shaped connector from the back (the welded connection does not appear on Figure 2) and extends downward, with the opening 5 cm above the bottom of the sample cell. Two small metal cylinders with a Viton O-ring between them were inserted in the NPT connection to the pressure head to make a vacuum seal. The adsorbent was covered with a 0.5-cm layer of glass chips to minimize heat loss through the top of the cell and regenerated *in situ*.

5. Thermopile Calibration

The primary calibration of the calorimeter (0.0540 W/mV) is based upon the Clapeyron equation[4] applied to a series of adsorption isotherms measured in a separate, high-precision volumetric apparatus for ethane on silicalite (MFI). The calibration constant for ethane was confirmed by excellent agreement of calorimetric data with the Clapeyron equation for SF_6, CO_2, and CH_4. The calibration constant is independent of the amount of adsorbent in the cell.

A secondary calibration based on electrical heating (0.059 W/mV) was 9% higher than the primary calibration. The voltage signal from the calorimeter was determined as a function of the rate of heat dissipation $dQ/dt = I^2R$ in a platinum resistance wire wrapped around the outside of the cell in thermal contact with the cell wall and the thermopiles. Similar difficulties were encountered by Handy et al.:[5] the voltage-to-power ratio for a resistor inside the cell was 9% lower than that for an externally wrapped resistance wire. The difference was attributed to heat losses. We chose the Clapeyron equation as the more reliable method of calibration.

6. Spurious Heat of Compression in Sample Cell

Before taking a measurement, the dosing loop and the sample cell are both at the temperature T_0 of the experiment; the pressure inside the sample cell is P_c, and the pressure in the dosing loop is some higher pressure P_d. Increments of gas are added to the sample cell by opening the valve between the dosing loop and the cell. The temperature of the gas inside the dosing loop falls

(4) Dunne, J. A.; Mariwala, R.; Rao, M.; Sircar, S.; Gorte, R. J.; Myers, A. L. *Langmuir* **1996**, *12*, 5888.

(5) Handy, T. L.; Sharma, S. B.; Spiewak, B. E.; Dumesic, J. A. *Meas. Sci. Technol.* **1993**, *4*, 1350.

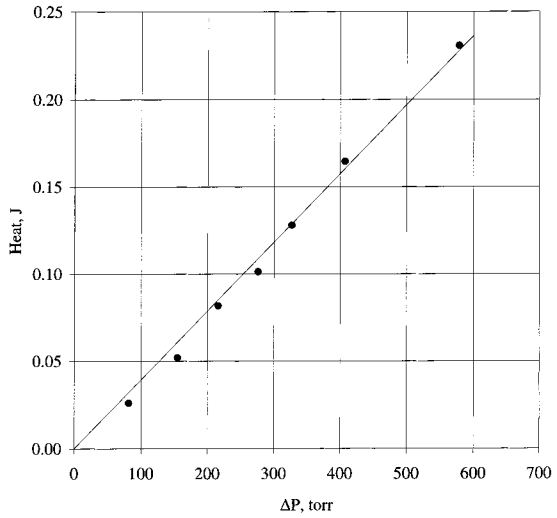

Figure 3. Linear correlation of a spurious sensible heat term for adding a dose of gas. The difference in pressure is the pressure in the dosing loop minus the pressure in the sample cell before opening the valve.

because of the expansion, while the temperature of the gas inside the sample cell rises as it is compressed by the incoming gas. The calorimeter measures both the latent heat of adsorption and the sensible heat liberated by the compressed gas as it cools to the temperature of the calorimeter. This sensible heat must be subtracted from the heat registered by the thermopiles to obtain the heat of adsorption.

The spurious heat term generated by compression of the gas inside the cell was determined by expanding gas from the dosing loop into a sample cell containing no adsorbent. For a 10-cm^3 dosing loop and for a dead space of 18 cm^3 in the sample cell, the linear correlation

$$Q_{sp} = a\Delta P \tag{12}$$

for the experimental data shown in Figure 3 is $a = 3.94 \times 10^{-4}$ J/Torr. ΔP is the driving force for the irreversible expansion: the pressure difference between the dosing loop and the sample cell.

The correlation ignores the effect of adsorption as gas enters the sample cell. For the case of weak adsorption, when only a small fraction of the gas entering the sample cell actually adsorbs, the neglect of adsorption is justified. For the case of strong adsorption, when most of the gas entering the sample cell adsorbs, the spurious heat of compression is negligible compared to the heat of adsorption. Thus, for strong adsorption (95% of gas dose adsorbs) or weak adsorption (5% of gas dose adsorbs), the approximation that the heat of compression is independent of adsorption is acceptable. We have no proof that the correction for the spurious heat of compression is negligible in the intermediate case when about 50% of the gas dose adsorbs, but the excellent agreement of both strong and weakly adsorbing gases with the Clapeyron equation is indirect evidence that eq 12 is adequate for both strongly and weakly adsorbing gases.

Other calorimeters[5] are designed for isothermal introduction of gas to the sample cell. This is accomplished by adding increments of gas slowly through a needle valve so that the temperature of the gas in the dosing loop is equal to the temperature in the sample cell (T_0). In the absence of adsorption, the reversible, isothermal introduction of a gas sample generates an exothermic heat inside the sample cell equal to RT_0 per mole of gas added; the signal for this spurious heat term can be nullified by adding the same amount of gas to a reference cell wired in reverse polarity. Isothermal dosing is effective for the measurement of heats of adsorption of pure gases. For mixtures, the fast, irreversible addition of increments of gas shortens the time required for mixing and equilibration.

7. RGA Calibration

The gas-phase composition is determined with a RGA, which is based on mass spectrometry. When a gas is admitted to the RGA, bombardment by electrons causes the molecules to fragment into positive ions of a whole series of masses. The relative abundance of ions of various masses is characteristic of the particular molecule. Compositions of gaseous mixtures can be determined by comparing their spectra with that of the pure compounds determined under the same conditions.

For a binary mixture, the calibration constant (K) of the RGA is based upon the relation

$$\frac{y_1}{y_2} = K\frac{I_1}{I_2} \tag{13}$$

where y_i is the mole fraction of component i in the gas phase and I_i is the intensity of the mass/charge ratio detected for a particular ion of that component. Equation 13 assumes that the contribution to the intensity I_1 is only due to component 1 and the intensity I_2 is only due to component 2. When both components of a binary mixture contribute to the intensity of a peak, the composition of the gas phase can still be determined by solving a system of equations for the intensity ratios.[6]

The intensity detected by the mass spectrometer is proportional to the flow rate of the gaseous molecules through the leak valve. At low pressure, the opening of the leak valve is small compared with the free mean path of the molecules. The resulting effusive flow of the gas is directly proportional to its partial pressure and inversely proportional to its molecular weight, so

$$\frac{I_1}{I_2} = \frac{Py_1}{Py_2}\left(\frac{M_2}{M_1}\right)^{1/2} \tag{14}$$

The mean free path decreases with pressure; at ≈100 Torr the mean free path is the same order of magnitude as the opening of the leak valve. When the ratio of the opening to the free mean path is in the range from unity to 100, the flow is intermediate between effusive and viscous.[7] For viscous flow, the composition of the gas leaving the cell and the intensity ratio obeys the simple relation

$$\frac{I_1}{I_2} = \frac{Py_1}{Py_2} \tag{15}$$

The transition from effusive to viscous flow is important for molecules having a large ratio of molecular weights, e.g., SF_6 (1) and CH_4 (2) with a molecular weight ratio of 9. In this case, the calibration "constant" K is a function of the pressure in the cell, as shown in Figure 4. For gases with smaller ratios of molecular weight, such as C_2H_4 and C_2H_6 with a ratio near unity, the calibration constant is effectively independent of pressure. Figure 5 shows

(6) Ewing, G. W. *Instrumental Methods of Chemical Analysis*, 3rd ed.; McGraw-Hill Book Company: New York, 1969; pp 394−400.
(7) Roth, A. *Vacuum technology*, 2nd ed.; North-Holland New York, 1982; p 63.

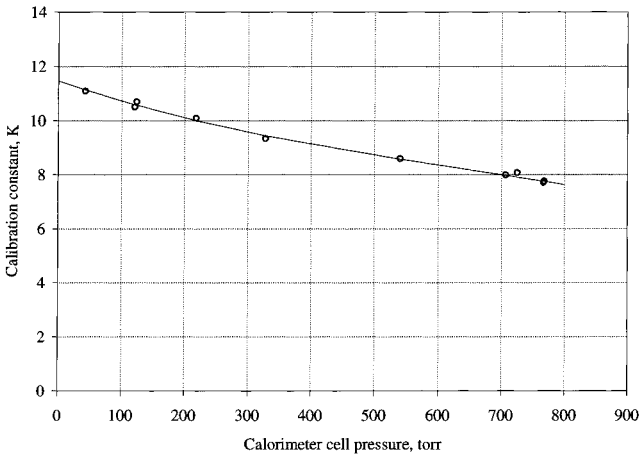

Figure 4. Effect of pressure on RGA calibration K of eq 15 for mixtures of SF_6 and CH_4.

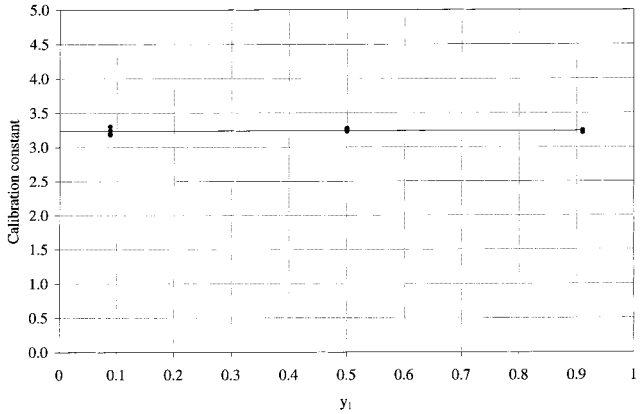

Figure 5. Calibration of the composition for mixtures of C_2H_4 and C_2H_6 based on eq 16. The calibration is independent of pressure.

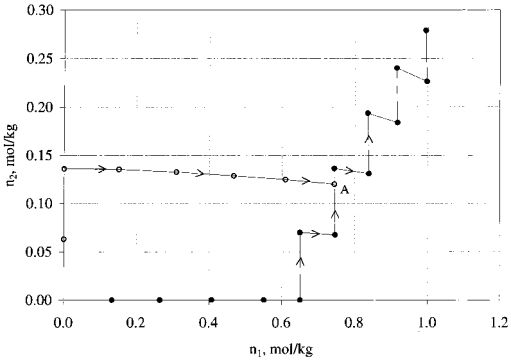

Figure 6. Loci of loading by alternate paths for mixtures of SF_6 and CH_4. Black circles and open circles indicate differnt paths which intersect at point A. Experimental data are given in Table 5 of the appendix.

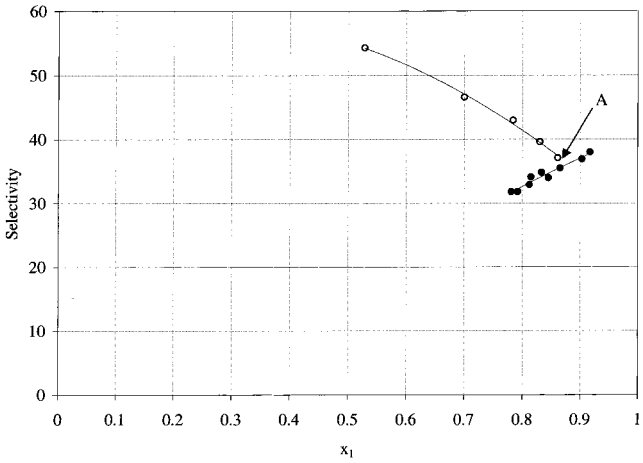

Figure 7. Selectivity of SF_6 relative to CH_4 at 21.5 °C. Symbols are the same as those in Figure 6. The selectivity at point A is independent of the order of contacting the components.

calibration data for C_2H_4 (component 1) and C_2H_6 (component 2). Both molecules contribute to the intensity I_{28} at $m = 28$, but only C_2H_6 contributes to the intensity I_{30} peak at $m = 30$, so

$$\frac{y_2}{y_1} = K_1 \frac{I_{30}}{I_{28} - K_2 I_{30}} \tag{16}$$

The average error in composition using the mass spectrometer is less than 1% for mid-range compositions. The lowest mole fraction that can measured is about 0.0005. The background noise is between 2 and 4 orders of magnitude smaller than the intensity of the peaks used to measure the compositions.

8. Verification of Adsorption Equilibrium

The mixing time required when a new dose of gas is added to the sample cell containing a gaseous mixture but no adsorbent is about 15 min.[2] Sampling the gas phase continuously to check for equilibrium is impracticable because the amount of gas sampled over 30 min would affect the mass balance used to calculate the amount adsorbed.

Two methods were used for verifying the attainment of equilibrium for mixture adsorption. The first method is to fit the experimental data to a model which is thermodynamically consistent; agreement of the model with the experimental data is an indirect but robust method of verifying equilibration. A second, direct method is to verify that a particular point is independent of the order of contacting the adsorbates. Figure 6 shows an example for the adsorption of mixtures of SF_6 (1) and CH_4 (2). The closed and open circles indicate two paths from zero loading to point A; the arrows show the direction of the paths. These two paths intersect at $n_1 = 0.78$ and $n_2 = 0.12$, or a mole fraction $x_1 = 0.87$. Figure 7 shows the selectivity for the same two paths; the selectivity curves intersect at $x_1 = 0.88$. Therefore, within an uncertainty of about 2%, the selectivity is independent of the order of contacting the adsorbates.

9. Determination of Differential Heats from Finite Doses

The amount dosed Δn must be small enough to measure the differential heat but large enough to generate an accurate heat signal Q. Because the differential heat is defined as the ratio of $Q/\Delta n$ in the limit as Δn goes to zero, the error associated with finite increments needs to be examined.

Assume that the differential heat $q_d(n)$ is given exactly by the polynomial:

$$q_d(n) = q_0 + d_1 n + d_2 n^2 + d_3 n^3 + \ldots \tag{17}$$

For a finite amount of gas adsorbed ($\Delta n = n_2 - n_1$), the approximate differential heat q_δ measured experimentally is

$$q_\delta = \frac{\int_{n_1}^{n_2} q_d(n)\, dn}{n_2 - n_1} \tag{18}$$

q_δ is the average value of the differential heat measured at the average loading $(n_1 + n_2)/2$. Comparison of q_δ with the exact differential heat at the same average loading gives the error:

$$q_\delta - q_d = \frac{d_2}{12}(n_1 - n_2)^2 + \frac{d_3}{8}(n_1 + n_2)(n_1 - n_2)^2 + ... \tag{19}$$

The error is of order $(n_1 - n_2)^2$. Because the leading term of the error is also proportional to the second derivative of the heat curve, $q_\delta = q_d$ for linear heat curves.

Figure 8 shows hypothetical differential (solid line) and integral (dashed line) heats of adsorption. The points show approximate heats q_δ calculated from eq 18 for finite doses $n_2 - n_1 = 0.1$, 0.5, and 1.0 mol/kg. Only for finite doses as large as 1 mol/kg can the difference between the exact differential q_d and the approximate q_δ be discerned. Typical experimental values of Δn are of order 0.1 mol/kg. Except for abrupt changes of heat with coverage associated with phase transitions, the error associated with using finite doses of gases to measure the differential heat is negligible.

It is convenient to report differential heats of adsorption at the loading n_2 instead of the average loading $(n_1 + n_2)/2$. This introduces errors larger than that predicted by eq 19, especially when the slope of the heat curve is large. Heats in Tables 3−5 of the appendix are reported at the final loading of n_2, which is justified for these systems because the heat profiles are practically horizontal lines and the increments Δn are small. Nevertheless, it is important to bear in mind that this approximation may not be valid for all cases.

10. Alternating Dosings of Each Component

Two independent dosings (A and B) are required to measure the individual differential heats of adsorption (q_1 and q_2) from a binary mixture:

$$Q^A = \Delta n_1^A q_1 + \Delta n_2^A q_2 \tag{20}$$

$$Q^B = \Delta n_1^B q_1 + \Delta n_2^B q_2 \tag{21}$$

where Q^A and Q^B are the heats registered by the calorimeter and Δn_1 and Δn_2 are the amounts adsorbed, or desorbed, of components 1 and 2, respectively. When the system of equations (20) and (21) is solved, the individual heats of adsorption are

$$q_1 = \frac{Q^A \Delta n_2^B - Q^B \Delta n_2^A}{\Delta n_1^A \Delta n_2^B - \Delta n_1^B \Delta n_2^A} \tag{22}$$

$$q_2 = \frac{Q^B \Delta n_1^A - Q^A \Delta n_1^B}{\Delta n_1^A \Delta n_2^B - \Delta n_1^B \Delta n_2^A} \tag{23}$$

Dosing of one component generates a positive incremental adsorption of that component which is normally 1 or 2 orders of magnitude larger than the accompanying desorption of the other component. The solution of eqs 22 and 23 requires that the dosing of the components be alternated; successive dosings of the same component generate an indeterminate solution. A sample calculation is given in the appendix.

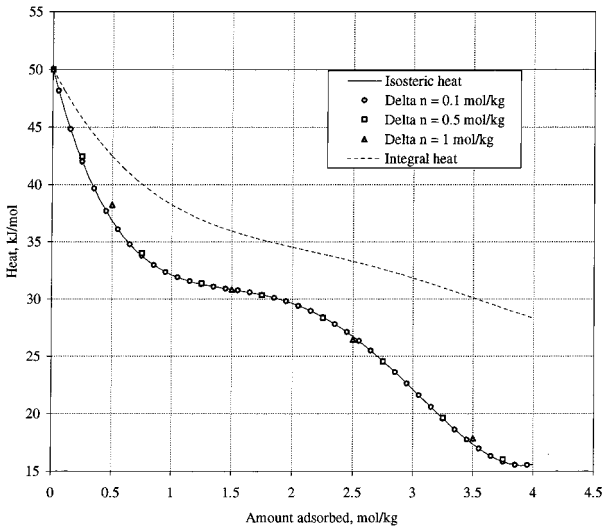

Figure 8. Comparison of the differential heat of adsorption (solid line) with experimental heats determined with finite doses of gas. The dashed line is the integral heat of adsorption. Heats determined experimentally with small doses of order 0.1 mol/kg agree very well with the exact differential heat.

11. Results and Conclusions

For presentation of experimental results, it would be helpful if one of the variables such as the total pressure or fugacity of one of the components could be held constant. However, the necessity of alternating doses generates a locus similar to the closed circles shown in Figure 6. The inability to obtain data along some locus such as an isobar is annoying but does not affect the analysis of the experimental data for activity coefficients and excess functions. After covering the entire phase diagram for a binary mixture by varying the preloading of the pure components, a model which fits the experimental data can be used to generate loci such as isobars or constant loading of one component.

Since our first measurements of heats of adsorption from binary mixtures reported in 1997[2] for CH_4 and C_2H_6 in silicalite and for CO_2 and C_2H_6 in NaX, we have completed experiments for four other binary mixtures; one of them is reported in this paper (SF_6 and CH_4 on NaX). Presently, we are computing thermodynamic excess properties for these mixtures, especially adsorbed-phase activity coefficients, excess free energy, excess entropy, and heat of mixing in the adsorbed phase. It is interesting that all of the excess functions are negative: activity coefficients are less than unity, and the heat of mixing is exothermic in every case.

Acknowledgment. This research was supported by Air Products and Chemicals, Inc., and by the National Science Foundation (NSF CTS 9610030).

Appendix. Sample Calculation

A sample calculation is illustrated for mixtures of SF_6 (1) and CH_4 (2). Tables 3 and 4 are the measurements for the pure components; Table 5 is for the mixture loci plotted in Figure 6. Table 2 shows a sample calculation of loading and heats of adsorption derived from the two points A and B indicated by italic type in Table 5. The incremental loading of component i for measurement j is calculated by the mass balance equation:

$$\Delta n_i^j = \frac{1}{RT}\left[V^d y_i^d \left(\frac{P^d}{z^d} - \frac{P^{df}}{z^{df}}\right) + V^c \left(\frac{P^{c,j-1} y_i^{c,j-1}}{z^{c,j-1}} - \frac{P^{c,j} y_i^{c,j}}{z^{c,j}}\right)\right]$$

Table 2. Experimental Data

variable	description	A	B
P^{d}	initial pressure in the dosing loop, Torr	352.6	303.0
P^{df}	pressure in the dosing loop after 2 min, Torr	84.90	97.39
$P^{c,j-1}$	pressure in the cell prior to dosing, Torr	15.58	85.08
$P^{c,j}$	pressure in the cell after dosing, Torr	85.08	91.41
y_1^{d}	composition of the gas in the dosing loop	0.000	1.000
$y_1{}^{c,j-1}$	composition of the gas in the cell prior to dosing	1.000	0.201
$y_1{}^{c,j}$	composition of the gas in the cell after equilibration	0.201	0.225
A	area (response from the thermopiles), mV·s	31.31	69.98
T	temperature, K	294.2	294.36
z^{d}	compressibility factor for the gas in the dosing loop prior to dosing	0.9992	0.9950
z^{df}	compressibility factor for the gas in the dosing loop after 2 min	0.9998	0.9984
$z^{c,j-1}$	compressibility factor for the gas in the cell prior to dosing	0.9997	0.9996
$z^{c,j}$	compressibility factor for the gas in the cell after dosing	0.9996	0.9996
V^{d}	dosing loop volume, cm^3	10.0	
V^{e}	cell volume, cm^3	17.853	
Δn_1	incremental amount adsorbed of component 1, mmol	−0.0015	0.1093
Δn_2	incremental amount adsorbed of component 2, mmol	0.0798	−0.0028
n_1^j	loading of component 1, mol/kg	0.6501	0.7460
n_2^j	loading of component 2, mol/kg	0.0700	0.0675
Q	total heat, $Q = KA$, J	1.691	3.779
Q_{sp}	spurious heat term, eq 12	0.133	0.086
$q_{d,1}^j$	differential heat of component 1, kJ/mol, eqs 19 and 20	34.3	
$q_{d,2}^j$	differential heat of component 2, kJ/mol, eqs 19 and 20	20.2	
$q_{st,1}^j$	isosteric heat of component 1, kJ/mol	36.7	
$q_{st.2}^j$	isosteric heat of component 2, kJ/mol	22.6	

Table 3. Adsorption of CH_4 on MFI

P, Torr	n, mmol/g	Q_{st}, kJ/mol	T, °C	P, Torr	n, mmol/g	Q_{st}, kJ/mol	T, °C
37.69	0.048	21.84	22.8	385.77	0.406		23.1
79.87	0.098	21.20	22.9	434.53	0.447	21.31	23.1
123.30	0.147		22.9	467.01	0.474	21.80	23.1
171.23	0.199	21.13	23.0	544.90	0.536	21.52	23.1
223.98	0.253	21.46	23.0	626.13	0.596	21.20	23.1
284.11	0.313		23.1	705.11	0.651	21.59	23.1
290.04	0.318	21.63	23.0	745.67	0.680		23.2
352.75	0.376	22.63	23.1	790.01	0.707	22.57	23.2
360.03	0.382	21.02	23.1	823.40	0.730	21.65	23.2

Table 4. Adsorption of SF_6 on MFI

P, Torr	n, mmol/g	Q_{st}, kJ/mol	T, °C	P, Torr	n, mmol/g	Q_{st}, kJ/mol	T, °C
2.21	0.131	35.81	23.5	140.87	1.541		24.1
5.21	0.270	36.52	23.6	164.60	1.586	39.18	24.0
9.06	0.411	36.31	23.7	188.00	1.620	39.01	24.1
13.21	0.536		23.7	259.35	1.692	39.31	24.2
13.46	0.540		23.7	350.11	1.747	40.06	24.1
18.63	0.667	36.24	23.7	455.34	1.786	41.84	24.2
25.34	0.800	36.13	23.7	527.14	1.814		24.0
33.75	0.933	36.44	23.8	571.84	1.816	41.06	24.1
44.91	1.072	36.41	23.9	626.87	1.832		24.1
60.11	1.212	36.76	23.9	688.40	1.836	40.28	24.2
82.06	1.351	37.24	23.9	726.44	1.847		24.0
115.64	1.480	38.52	23.9	804.39	1.852	36.87	24.2

The total loading of component i is $n_i^j = n_i^{j-1} + \Delta n_i^j/w$, where w is the mass of adsorbent (1.1406 g). The spurious heat term Q_{sp} calculated from eq 13 is subtracted from Q^A and Q^B before calculating the differential heats from eqs 19 and 20. The thermopile calibration constant is $K = 0.0540$ W/mV.

Table 5. Adsorption of Mixtures of SF_6 and CH_4 on MFI

P, Torr	T, °C	y_1	x_1	n, mmol/g	$Q_{st,1}$, kJ/mol	$Q_{st,2}$, kJ/mol	$S = (x_1/y_1)/(x_2/y_2)$
1.96	20.9	1.000	1.000	0.133			
4.41	20.9	1.000	1.000	0.265	34.56		
7.75	21.0	1.000	1.000	0.407	34.20		
12.00	21.0	1.000	1.000	0.551	35.49		
15.58	21.0	1.000	1.000	0.651	35.31		
85.08	*21.1*	*0.201*	*0.903*	*0.720*	*35.14*	*22.57*	*36.9*
91.41	*21.2*	*0.225*	*0.917*	*0.814*	*36.74*	*22.60*	*38.0*
172.50	21.4	0.138	0.845	0.880	36.74	22.39	34.0
183.29	21.4	0.152	0.865	0.970	35.74	22.35	35.5
270.19	21.5	0.116	0.812	1.029	35.76	22.66	32.9
283.51	21.5	0.126	0.833	1.101	35.67	22.66	34.8
366.36	21.5	0.107	0.792	1.155	35.62	22.19	31.8
384.81	21.5	0.114	0.815	1.224	35.91	22.21	34.1
475.41	21.5	0.101	0.781	1.273	35.98	22.71	31.8
49.70	22.4	0.000	0.000	0.063		21.30	
111.90	22.5	0.000	0.000	0.136		20.68	
114.95	21.3	0.020	0.528	0.287	34.32	20.32	54.3
121.95	21.3	0.048	0.700	0.442			46.6
130.83	21.5	0.078	0.784	0.596			43.0
140.97	21.6	0.110	0.830	0.735			39.6
153.05	21.8	0.143	0.861	0.864			37.1

LA980946A